

# Flavor-dependent EMC effect from a nucleon swelling model

Rong Wang<sup>1,\*</sup>, Raphaël Dupre<sup>1</sup>, Silvia Niccolai<sup>1</sup>, Yin Huang<sup>2</sup>, and Baiyang Zhang<sup>3</sup>

<sup>1</sup> *Institut de Physique Nucléaire, CNRS-IN2P3, Univ. Paris-Sud,  
Université Paris-Saclay, 91406 Orsay Cedex, France*

<sup>2</sup> *School of Physics and Nuclear Energy Engineering,  
International Research Center for Nuclei and Particles in the Cosmos  
and Beijing Key Laboratory of Advanced Nuclear Materials and Physics,  
Beihang University, Beijing 100191, China and*

<sup>3</sup> *Wigner Research Center for Physics, H-1121 Budapest, Hungary*

(Dated: May 16, 2019)

We present the flavor-dependent EMC effect from nIMParton nuclear PDFs, of which the  $x$ -dependence is described with a nucleon swelling model. The nuclear correction originated from the nucleon swelling is considered through modifying the initial valence quark distributions instead of the dynamical rescaling. To probe the flavor-dependence of the model, the experimental observables are calculated applying nIMParton nuclear modifications for the widely discussed experiments: parity-violating deep inelastic scattering on nuclear target, pion-induced Drell-Yan experiment, and  $W$ -boson production in proton-nucleus collisions. In addition, we show that measuring the spectator-tagged deep inelastic scattering process is another novel experimental method to probe the flavor-dependent EMC effect, which can be performed on CLAS12 with ALERT detector. The predictions of  $F_2$  ratios for bound proton and bound neutron are given for the future experimental test.

## I. INTRODUCTION

Since the discovery of the EMC effect [1], it has become a frontier for both the particle and the nuclear physics communities to understand the modification of short-distance structure by the presence of the nuclear medium or the neighboring nucleons. It has been a consensus that the EMC effect is ascribed to the nonperturbative mechanism of strong interaction. However the underlying Quantum Chromodynamics (QCD) theory is unsolvable in the respect of the interaction of average inter-nucleon distance. Nonetheless, a tremendous amount of models are raised to understand the EMC effect with decades of efforts (some reviews, Refs. [2–7]). Generally all the models describe fairly good the main features of the EMC effect. Other details about the EMC effect is crucial and necessary to constrain the models and to pin down the particular origin of the EMC effect.

Up to now, the  $x$ -dependence, the  $Q^2$ -dependence, and the nuclear dependence of the EMC ratios are investigated under a large number of experimental measurements. Basically all the models depict well the  $x$ -dependence of the EMC ratios. The  $Q^2$ -dependence of structure function ratio is found to be weak in experiments, and the  $Q^2$ -dependence of nuclear parton distribution functions (PDFs) obeys the QCD-based DGLAP evolution which governs the  $Q^2$ -dependence of free nucleon PDFs as well [8–10]. The recent measurement of the nuclear dependence of the EMC effect at JLab [11] implies that the EMC effect dominantly originates from the high virtuality or the high local density [5, 6, 12, 13]. The detailed study of the flavor-dependence of the EMC

effect is one of the next directions for future experiments [7, 14–16]. Investigating the variations of the nuclear medium modifications for quarks of different flavors opens a new window to test the various models.

The CBT model [14, 17–19] is the first model to bring out the nuclear effect difference between up quark and down quark. In CBT model, the nuclear PDFs are determined using a confining Nambu-Jona-Lasinio model, where the nucleon is approximated as a quark-diquark bound state in the Faddeev equation [17]. The nuclear effect is implemented with the scalar and vector mean fields coupling to the quarks, and the strength of the mean-fields are self-consistently determined using an equation of state for nuclear matter. The isovector-vector mean field  $\rho^0$  arisen from neutron or proton excess in nuclei breaks down  $u_p(x) = d_n(x)$  and  $d_p(x) = u_n(x)$  for bound nucleons, resulting in the flavor-dependence of the EMC effect.

Recently, nIMParton (nuclear “IM Parton”) global analysis studied the nuclear parton distributions with a nonperturbative input which consists of only three valence quarks [20, 21]. Instead of adding degrees of freedom from nuclear physics, the EMC effect in nIMParton analysis is produced from the deformation of valence quark distributions at the input scale  $Q_0^2$  due to the mechanism of nucleon swelling. The influence of the nuclear interactions or the mean-field mesons are all reflected in the nucleon swelling in the model. According to the Heisenberg uncertainty principle, the larger nucleon size gives rise to smaller widths of the momentum distributions of partons. The nuclear PDFs at high  $Q^2$  are then dynamically generated from the QCD-based evolution [20]. The nIMParton nuclear modification factors for up, down and strange quarks present some differences. There are no initial strange quarks at the input scale  $Q_0^2$ . All the strange quarks are generated from gluon splitting

\* wangrong@ipno.in2p3.fr

in QCD evolution. This is why the nuclear medium modification of strange quark distribution is different from that of valence quarks. The nuclear modifications of up and down quarks manifest some difference, and it is due to the width difference between the up valence quark distribution and the down valence quark distribution. Inside the proton, the width of down valence quark distribution is narrower than that of up valence quark distribution. With the same size of the increment of nucleon radius, the down valence quark distribution deforms more greatly to meet the condition of Heisenberg uncertainty principle.

On the experimental side, several high energy scattering processes are suggested to observe the flavor-dependence of the EMC effect [14–16]. They are the parity-violating deep inelastic scattering (PVDIS) process with a polarized electron beam [14], the pion-induced Drell-Yan (DY) processes with pion beams [15], and the W-boson production with high energy proton-nucleus collisions [16]. In these experiments, the sensitivities to the flavor-dependence of the EMC effect are all discussed under the CBT model. It is worthwhile and important to see also the predictions from other models. In this paper, we show the predicted experimental observables of above experiments using the flavor-dependent nuclear effect from nIMParton nuclear PDFs. Although the flavor-dependence of nIMParton nuclear modification is weak, it provides a baseline to understand the nuclear isovector force in CBT model.

A comprehensive physics program to investigate the nucleon structure of  ${}^4\text{He}$  is proposed with the idea of detecting the low energy recoil nuclei using A Low Energy Recoil Tracker (ALERT) combined with the CLAS12 detector at JLab [22–24]. The helium-4 nucleus has a density and a binding energy comparable to that of heavier nuclei, which is a typical target of interests in understanding the nuclear medium effect. By tagging the nuclear spectator, the ALERT experiment will access the additional information about the bound nucleon virtuality, which can provide the opportunity to clearly differentiate the many models describing the EMC effect [24]. With the spectator tagged, one knows the type of the nucleon struck by the high energy probe. The EMC effect of the bound proton and the bound neutron can be measured, which could shed some lights on the isospin-dependence of the EMC effect. In this work, we predict the EMC effect difference between the nuclear medium modified proton and the nuclear medium modified neutron based on nIMParton PDFs. The nucleus recoil-tagged deep inelastic scattering (DIS) off nuclear target is a new way to have a glance of the flavor-dependent EMC effect.

In Sec. II, we review the nucleon swelling model used to explain the EMC effect. The size of nucleon swelling obtained from nIMParton analysis is compared with the experimental measurements and the model calculations. The nIMParton analysis based on the nucleon swelling and the flavor-dependence of the nuclear effect are introduced in Sec. III. The experimental observables of

PVDIS process, pion-induced DY process and p-A collisions are shown in Sec. IV, Sec. V and Sec. VI respectively, applying nIMParton nuclear PDFs. In Sec. VII, we discuss the potential of tagged-DIS to probe the flavor-dependence of the EMC effect. Lastly, a brief summary is given in Sec. VIII.

## II. NUCLEON SWELLING AND THE EMC EFFECT

The models of the EMC effect are roughly classified into two categories: conventional nuclear physics models and the QCD-inspired models [2]. The conventional nuclear models usually take into account the reduced nucleon mass in medium or the virtuality, which gives the  $x$ -rescaling models [25–30] ( $x = Q^2/(2m_N\nu)$ ) and the off-shellness corrections [31–35]. The QCD-inspired models usually require an increase of the quark confinement, or a simple increase of nucleon radius (nucleon swelling). A bigger nucleon means a higher resolution power for the probe. In the language of QCD evolution, the  $Q^2$ -rescaling [36–40] (an higher resolution scale) are carried out to interpret the effect.

The nucleon swelling discussed in this work refers to the increase of the quark confinement size. There is no doubt that the charge radius of the nucleon is closely related to the average confinement of up and down valence quarks. The quark confinement enlargement is commonly understood in the multi-quark cluster model or a tiny quark deconfinement [41–45], the Quark-Meson Coupling (QMC) model [46–48], and the nuclear potential model [54–56]. In the multi-quark cluster model, the heavy nuclei favor the formations of multi-nucleon clusters containing  $3N$  ( $N = 1, 2, 3, \dots$ ) valence quarks. A small part of  $3N$ -quark configurations creates enlarged confinement on average. In the QMC model, the size of the non-overlapping nucleon bag changes with the exchange of the mean-field meson. In the potential model, the three-quark quantum system are modified by the nuclear attractive potential.

While it is difficult to quantify the strength of nucleon swelling, there are a few experiments which imply an increase of the quark confinement radius in the nuclear medium [49–52]. The nucleon swelling is found to be small for the Helium-3 nucleus through a quasi-elastic scattering experiment, which is smaller than 3-6 percent-age [49]. The other experiment with kaon probe hints that around 20% increase of the confinement range is possible for  ${}^{12}\text{C}$  and  ${}^{40}\text{Ca}$  [50]. Furthermore, an interesting analysis of the data of hadron-nucleus interaction shows that the effective cross section with bound nucleon is slightly larger than that with free nucleon, which implies the confinement increase [53].

In nIMParton analysis, the increments of the nucleon size are obtained from a global analysis to the nuclear DIS data from worldwide facilities. A large increase of nucleon size is not needed to produce the observed EMC

effect based on the analysis. The swellings of the nucleon radius are estimated to be 0.8%, 2% and 8% for deuteron,  $^3\text{He}$  and  $^{208}\text{Pb}$  respectively [20] in nIMParton global fit. The confinement size of valence quarks is reluctant to change with the nuclear environment. The size of nucleon swelling from experiments and from various models are listed in Table I. Some models predict just a few percentage of nucleon swelling as well, such as the QMC model [48], the binding potential model [54], the Skyrmion model [55], the quark-nucleon interaction model [56], the chiral quark-soliton model [57], the chiral symmetry restoration model [58], the weak stretching model [59], the PLC-suppression model [60], and the statistical model [61].

TABLE I. The magnitudes of nucleon swelling inferred from experiments and predicted from various models.

experiment/model	size of nucleon swelling
quasielastic scattering [49]	< 3 – 6% for $^3\text{He}$
$\text{K}^+$ -nucleus scattering [50]	10 – 30% for $^{12}\text{C}$ and $^{40}\text{Ca}$
nIMParton [20]	2.0 – 8.1% for $^3\text{He}$ - $^{208}\text{Pb}$
QMC [48]	5.5% for typical nuclei
binding potential [54]	a few % for typical nuclei
Skyrmion model [55]	3 – 4%
quark-N interaction [56]	$\sim 2\%$ for nuclear matter
chiral quark-soliton [57]	$\sim 2.4\%$ for heavy nuclei
chiral symmetry [58]	< 10% for nuclear matter
N-N overlapping [37]	4.7 – 22% for $^3\text{He}$ - $^{208}\text{Pb}$
weak stretching [59]	4.5 – 9.4% for $^4\text{He}$ - $^{208}\text{Pb}$
PLC-suppression [60]	1 – 3%
statistical model [61]	2.2 – 5.0% for $^4\text{He}$ - $^{197}\text{Au}$
quark-quark correlation [62]	15%
chiral quark-meson [63]	$\sim 19\%$ for nuclear matter
string model [64]	40%

Regardless of the origin of nucleon swelling, the valence quark distributions are redistributed according to uncertainty principle to adapt for a larger confinement in nIMParton analysis [20], instead of the dynamical rescaling [36–40]. In the nucleon swelling model, all the medium modifications are reflected in the simple picture of an increase of quark confinement radius. The input of three nearly free valence quarks sense the bigger “bag” of the nucleon, and change the widths of momentum distributions accordingly (see Eq. (6) and Fig. (2) in Ref. [20]). For the current nIMParton analysis, the swellings of the bound proton and the bound neutron are identical, and the up and down valence quarks are confined in the same enlarged space. The flavor-dependence of the EMC effect comes from the simple fact that the widths of up and down valence quark distributions are different. The width of the momentum distribution of down valence quark is narrower than that of up valence quark, and the PDF ratio of down valence quark is more sensitive to the swelling. The flavor-dependence of the nuclear modification factor is mainly in the range of  $0.1 < x < 0.4$  (See Fig. 7 in Ref. [20]).

### III. NIMPARTON NUCLEAR PARTON DISTRIBUTION FUNCTIONS

The nIMParton global analysis takes the nonperturbative input of three valence quarks and the DGLAP evolution with parton-parton recombinations [20]. The nucleon swelling effect is applied to the initial three valence quark distributions to describe the EMC effect. For the current nIMParton, the nucleon swelling factor is the same for all the nucleons inside a nucleus, and for the partons of all flavors. No direct effects of virtual mean-field mesons are taken to calculate the nuclear quark distributions in nIMParton analysis. A sophisticated nuclear-dependence is modeled with only two free parameters. Therefore the nuclear modifications are give as well for the unmeasured nuclei from nIMParton [20, 21].

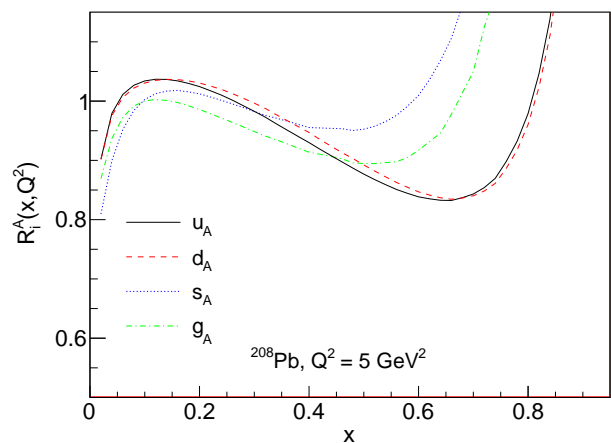


FIG. 1. Nuclear modification factors of different flavors from nIMParton [20, 21] are shown.  $R_i^A$  here is defined as  $Af_i^A/[Zf_i^p + Nf_i^n]$ , in which  $f_i^A$  is calculated with Eq. (1).

The nIMParton nuclear PDFs are from the global analysis to the DIS data of various nuclear targets, within the framework of three valence quarks input and nucleon swelling prescription [20, 21]. The flavor-dependence of the EMC effect for bound proton is shown in Fig. 7 of Ref. [20], which is weak but clear. Inside the bound proton, the EMC effect of down quark is stronger than that of up quark. The nuclear PDF of flavor  $i$  can be calculated from the nIMParton nuclear modification factors with the following formula,

$$f_i^A(x, Q^2) = \left[ ZR_i^{\text{bound } p}(x, Q^2)f_i^p(x, Q^2) + (A - Z)R_i^{\text{bound } n}(x, Q^2)f_i^n(x, Q^2) \right] / A, \quad (1)$$

where  $Z$ ,  $A$ ,  $f_i^A(x, Q^2)$ ,  $f_i^p$  and  $f_i^n$  are atomic number, mass number, nuclear PDF, proton PDF and neutron PDF respectively. The nuclear modifications  $R_i^{\text{bound } p}(x, Q^2)$  and  $R_i^{\text{bound } n}(x, Q^2)$  can be accessed from the web [21]. For the calculations in this paper, the isospin symmetry is assumed for bound proton and

bound neutron, which implies  $f_u^n = f_d^p$ ,  $f_d^n = f_u^p$ ,  $f_{\bar{u}}^n = f_{\bar{d}}^p$  and  $f_{\bar{d}}^n = f_{\bar{u}}^p$ .

The nuclear modification factors using Eq. (1) are shown in Fig. 1. The differences among the ratios indicate the flavor-dependence of the nuclear medium effect. Under the nIMParton data set, the differences are large among the ratios of valence quark distribution, sea quark distribution, and gluon distribution while the nuclear modification difference is small for up quark distribution and down quark distribution in a nucleus, showing the maximum around  $x = 0.5$ . The anti-shadowing of gluon and sea quarks are not obvious, which are consistent with the Drell-Yan data. Basically, there are no enhancements of nuclear anti-quark distributions shown in E772 [65] and E866 data [66] of the DY di-muon production at Fermilab in the range of  $0.01 < x < 0.3$ .

#### IV. PARITY-VIOLATING DEEP INELASTIC SCATTERING

By using the polarized electron probe, the parity-violating DIS experiment under high luminosity would present an important test on the difference between the EMC effect of up quark and that of down quark [14]. This experimental idea to check the flavor-dependent modifications of nuclear medium is to measure the difference between the traditional  $F_2$  ratio and the  $\gamma Z$  interference structure function ratio. The ratio definitions of the EMC effect for both the traditional DIS and the  $\gamma Z$  interference structure functions are written as,

$$R^i = \frac{F_{2A}^i}{F_{2A}^{i,naive}} = \frac{F_{2A}^i}{ZF_{2p}^i + NF_{2n}^i}, \quad (i = \gamma, \gamma Z) \quad (2)$$

where  $F_{2A}^\gamma$  and  $F_{2A}^{\gamma Z}$  are the traditional unpolarized structure function and the  $\gamma Z$  interference structure function respectively. The dominant term of the cross-section asymmetry between the positive and the negative electron helicity is denoted as  $a_2$  [14], which is directly connected to the ratio of  $F_{2A}^\gamma$  and  $F_{2A}^{\gamma Z}$ . Therefore the  $F_{2A}^{\gamma Z}$  can be extracted combining the  $a_2$  measurement of PVDIS and the traditional  $F_{2A}$  data.

Fig. 2 shows the  $a_2$  of Lead using only up and down quark distributions with the application of nIMParton nuclear modification factors. The calculations of  $a_2$  are given with the formula in Ref. [14], which assumes  $s + \bar{s} \ll u + d + \bar{u} + \bar{d}$ . One can find that the  $a_2$  value actually depends on the PDF set used. Nevertheless, both PDF sets show small changes of  $a_2$  curves using nIMParton nuclear modifications, which is different from the prediction of CBT model. There is an obvious difference between the naive  $a_2$  and the  $a_2$  with CBT nuclear correction [14]. Moreover, the  $x$ -dependence of  $a_2$  of  $^{208}\text{Pb}$  predicted from CBT model and that from nIMParton nuclear PDFs show clearly different behaviors. The  $a_2$  curve applying nIMParton nuclear PDFs is rather flat, while the  $a_2$  curve goes up quickly with  $x$  approaching

one in the CBT model (see Fig. 1 in Ref. [14]). Fig. 3 shows  $a_2$  of Lead with strange quark distribution included. Adding strange quark distribution changes much  $a_2$  in small  $x$  region only. Therefore the  $a_2$  measurement in the valence region is feasible to distinguish the different models about the flavor-dependent EMC effect.

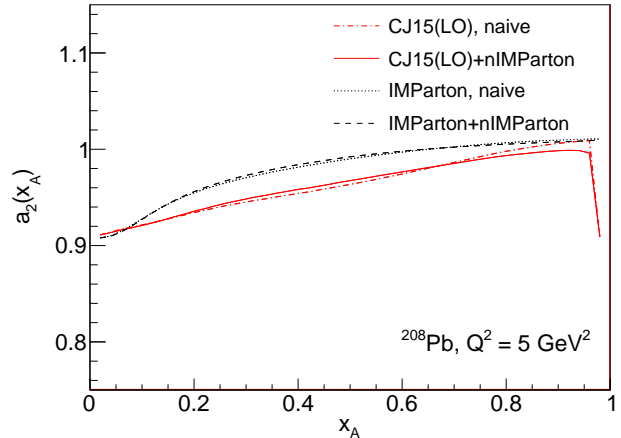


FIG. 2. The  $a_2$  term of the analyzing power of longitudinally polarized electron DIS scattering on  $^{208}\text{Pb}$  target. In the calculations, the strange quark distribution and the heavy quark distributions are neglected. CJ15(LO) PDF is taken from Refs. [68, 69]. IMParton PDF is taken from Refs. [70, 71]. nIMParton nuclear correction factor is from Refs. [20, 21].

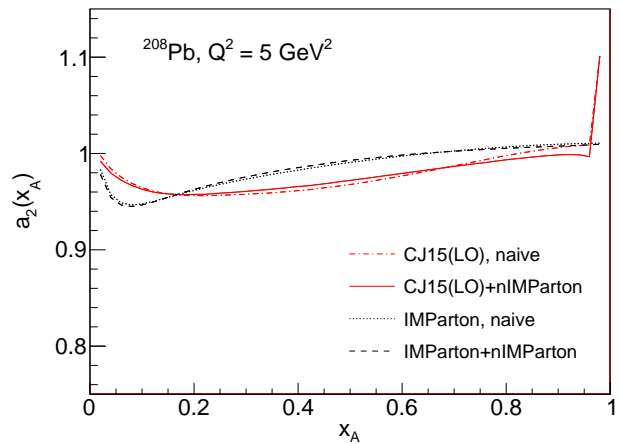


FIG. 3. The  $a_2$  term of the analyzing power of longitudinally polarized electron DIS scattering on  $^{208}\text{Pb}$  target. Up, down, and strange quark distributions are all used in the calculations. CJ15(LO) PDF is taken from Refs. [68, 69]. IMParton PDF is taken from Refs. [70, 71]. nIMParton nuclear correction factor is from Refs. [20, 21].

Fig. 4 shows the comparisons between the traditional structure function ratio and the  $\gamma Z$  interference structure function ratio. The formula to calculate these structure

functions in terms of up and down quark distributions can be found in Ref. [14]. Based on the nIMParton nuclear modifications, the difference between  $R_{Lead}^\gamma$  and  $R_{Lead}^{\gamma Z}$  is trivial. This conclusion is clearly different from that predicted by CBT model. The CBT model predicts a noticeable difference between  $R_{Lead}^\gamma$  and  $R_{Lead}^{\gamma Z}$  based on the flavor-dependent nuclear force (the  $\rho_0$  mean field). The data points in Fig. 4 show the extrapolated EMC ratios for infinite nuclear matter [67]. The heavy nucleus  $^{208}\text{Pb}$  can be viewed as the infinite nuclear matter approximately. The predictions by nIMParton are consistent with the data. The  $R_{Lead}^{\gamma Z}$  extracted from PVDIS experiment is of significance to check the predictions of the general nucleon swelling effect and of the isovector field effect.

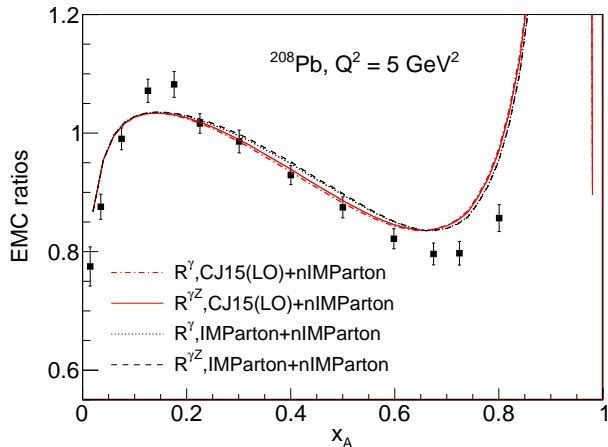


FIG. 4. The traditional DIS and the  $\gamma Z$  interference structure function ratios of  $^{208}\text{Pb}$  to free nucleons. In the calculations, the strange quark distribution and the heavy quark distributions are ignored. CJ15(LO) PDF is taken from Refs. [68, 69]. IMParton PDF is taken from Refs. [70, 71]. nIMParton nuclear correction factor is from Refs. [20, 21]. The square points depict an extrapolation for infinite nuclear matter using a local density approximation [67].

## V. PION-INDUCED DRELL-YAN PROCESS

Pion-induced Drell-Yan process is also a sensitive experimental tool to probe the flavor-dependent EMC effect [15]. The DY cross section ratios which are sensitive to the nuclear up and down quark distributions are denoted as,

$$\begin{aligned}
 R_{\pm}^{DY} &= \frac{\sigma^{DY}(\pi^+ + A)}{\sigma^{DY}(\pi^- + A)} \approx \frac{d_A(x)}{4u_A(x)} \\
 R_{-}^{DY,A/D} &= \frac{\sigma^{DY}(\pi^- + A)}{\sigma^{DY}(\pi^- + D)} \approx \frac{u_A(x)}{u_D(x)} \\
 R_{-}^{DY,A/H} &= \frac{\sigma^{DY}(\pi^- + A)}{\sigma^{DY}(\pi^- + H)} \approx \frac{u_A(x)}{u_p(x)}
 \end{aligned} \quad (3)$$

where A, D, and H represent the nuclear, the deuteron and the hydrogen targets respectively.  $R_{\pm}$  measures the nuclear down quark to up quark ratio, while  $R^-$  measures the nuclear medium modification of up quark distribution. The precise data of these DY cross-section ratios would provide some stringent constraints to various models on the EMC effect.

The comparisons between the predictions from nIMParton nuclear modifications and the existing pionic DY data are shown in Fig. 5. The upper panels indicate that the nIMParton nuclear modifications describe well the EMC effect of up quark distribution for both Tungsten and Platinum targets. From the lower panels, we find that the nIMParton nuclear modifications may not describe well the nuclear down quark to up quark ratios. However the uncertainties of the  $R_{\pm}$  data are quite big up to date. The CBT model successfully interpret well all the data except the NA10 data (see Fig. 2 in Ref. [15]). We need the possible future pion-induced Drell-Yan experiments to test the predictions and to quantify the flavor-dependence of the EMC effect.

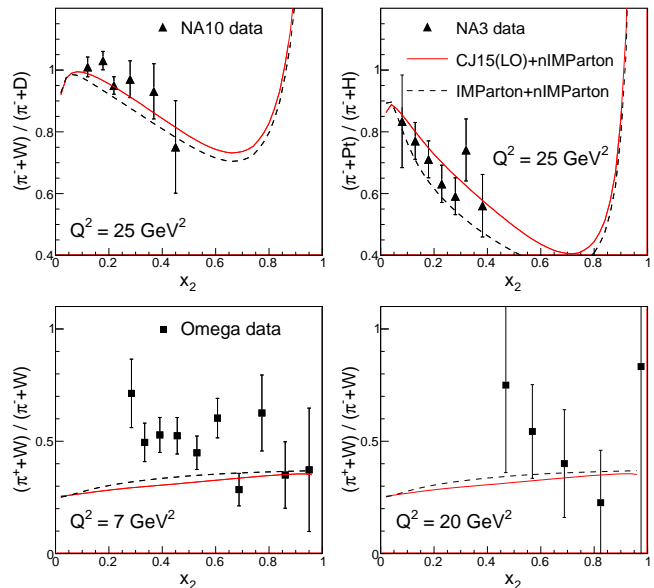


FIG. 5. The ratios between the cross-sections of different pion-induced Drell-Yan processes. CJ15(LO) PDF is taken from Refs. [68, 69]. IMParton PDF is taken from Refs. [70, 71]. nIMParton nuclear correction factor is from Refs. [20, 21]. The triangles represent the NA10 [72] and NA3 [73] data. The squares represent the Omega data [74].

## VI. W BOSON PRODUCTION IN PROTON-NUCLEUS COLLISIONS

Chang et al. suggest that it is another possible method to explore the flavor-dependent EMC effect by measuring the differential cross-sections of W boson production in proton-nucleus collisions [16]. The experimental ob-

servables related to the topic are the cross-section ratios which are defined as the followings,

$$\begin{aligned}
 R_{A/D}^+(x_F) &= \frac{\frac{d\sigma}{dx_F}(p + A \rightarrow W^+ + X)}{\frac{d\sigma}{dx_F}(p + D \rightarrow W^+ + X)} \approx \frac{u_A(x_2)}{u_D(x_2)}, \\
 R_{A/D}^-(x_F) &= \frac{\frac{d\sigma}{dx_F}(p + A \rightarrow W^- + X)}{\frac{d\sigma}{dx_F}(p + D \rightarrow W^- + X)} \approx \frac{d_A(x_2)}{d_D(x_2)}, \\
 R_{A/D}^\pm(x_F) &= \frac{\frac{d\sigma}{dx_F}(p + A \rightarrow W^+ + X)}{\frac{d\sigma}{dx_F}(p + A \rightarrow W^- + X)} \approx \frac{\bar{d}_p(x_1)u_A(x_2)}{\bar{u}_p(x_1)d_A(x_2)},
 \end{aligned} \tag{4}$$

in which  $x_F = x_1 - x_2$  is the Feynman  $x$  variable of the  $W$  boson,  $x_1$  and  $x_2$  are the momentum fractions carried by the partons in the initial proton and in the initial nucleus respectively.  $A$  and  $D$  denote the heavy nucleus and the deuteron respectively.

Fig. 6 shows the predictions of the cross-section ratios of  $W$  boson production in different models for the proton-Lead collisions. The  $Q$  scale of the parton model calculations is chosen to be the  $W$ -boson mass scale. It is interesting to find that the result based on the nuclear medium correction of nIMPArton is between that of CBT model and that of CBT model without the isovector meson force. These different model predictions can be verified with the apparatuses at LHC or RHIC in the runs of high energy proton-nucleus collisions under high luminosities.

## VII. SPECTATOR-TAGGED DEEP INELASTIC SCATTERING

Spectator-tagged DIS from deuterium and  $^4\text{He}$  are proposed to be measured using CLAS12 detector combined with ALERT detector specialized in detecting the low energy spectator nuclei [24]. By tagging the nuclear recoil spectators ( $^4\text{He}(e, e^{\prime 3}\text{H})X$  and  $^4\text{He}(e, e^{\prime 3}\text{He})X$ ), we can probe the nuclear effect difference between the bound proton and the bound neutron. The experiment measuring medium modified nucleons would provide some novel and important tests on many models describing the EMC effect.

Measurement in the deep inelastic region accesses the structure functions of nucleons. In the leading order and ignoring the contributions of heavy quarks, the proton structure function is expressed as  $F_2^p = \frac{4}{9}u^p + \frac{1}{9}d^p + \frac{1}{9}s^p$ . Under the assumption of isospin symmetry, the neutron structure function is expressed as  $F_2^n = \frac{4}{9}u^n + \frac{1}{9}d^n + \frac{1}{9}s^n = \frac{4}{9}d^p + \frac{1}{9}u^p + \frac{1}{9}s^p$ . It is easy to find that the flavor-dependence of the nuclear modifications on quark distributions could result in the difference of the EMC effect between medium modified proton and medium modified neutron. If the nuclear modifications on up and down quarks are the same, then the EMC ratios for bound proton and bound neutron are identical (ignoring the contribution of strange quark in the large  $x$  region).

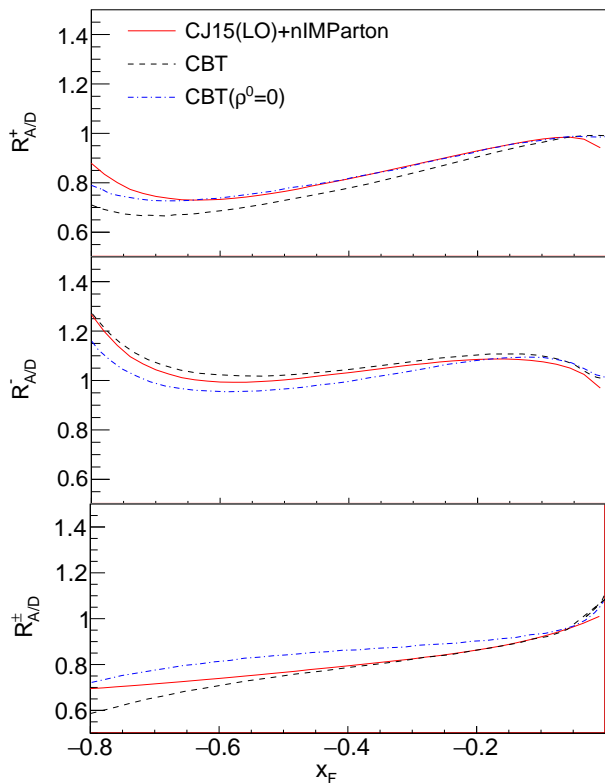


FIG. 6. nIMPArton predictions of the cross-section ratios of  $W$  boson productions for proton-nucleus collisions (between  $^{208}\text{Pb}$  and deuteron, see text for explanations) with the center-of-mass energy of  $\sqrt{s} = 5.520$  TeV, compared with the CBT model [17–19]. CJ15(LO) PDF is taken from Refs. [68, 69]. nIMPArton nuclear correction factor is from Refs. [20, 21].

Fig. 7 shows the EMC effects of bound proton and bound neutron inside the  $^4\text{He}$  nucleus. In the calculations, the nuclear modifications on parton distributions are taken from nIMPArton analysis [20, 21]. The EMC ratios for bound proton and for bound neutron exhibit some differences, especially around  $x = 0.5$ . Therefore, the tagged-DIS experiment has the potential to test nIMPArton prediction and the nucleon swelling model used to soften the valence quark distributions. To quantify the EMC effect of the bound neutron, the free neutron structure function data is needed as the reference. Fortunately, the state-of-the-art measurement of the nearly free neutron structure function is currently realized by the BoNUS Collaboration at JLab [75–77].

To clearly demonstrate the magnitude difference of the EMC effect between the bound proton and the bound neutron, The ratio of the nuclear EMC effect is shown in Fig. 8. It is shown that at  $x$  around 0.5, the difference between the EMC ratios of the bound proton and bound neutron is at the maximum of about 3% relatively. The ALERT project will be able to explore the variation of the nuclear modification within the statistical error bars of 1 to 2% [24]. Hence, the ALERT detector with CLAS12



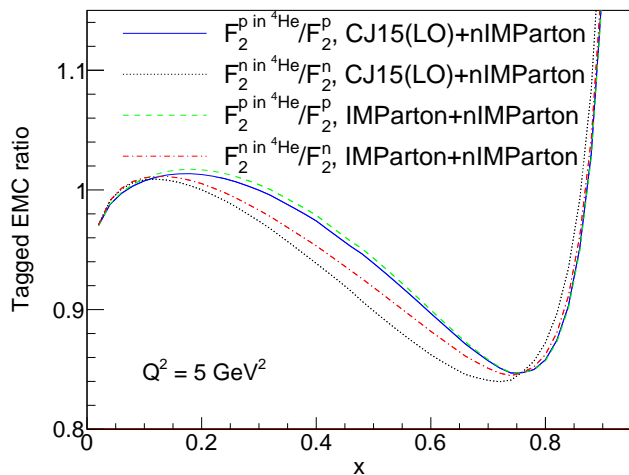


FIG. 7. Predictions of the spectator-tagged EMC ratios for  ${}^4\text{He}$  nucleus. The PDFs of free proton and free neutron are taken from CJ15 [68, 69] and IMParton [70, 71]. The nuclear modifications of PDFs in bound nucleons are adopted from nIMParton global analysis [20, 21]. The  $Q^2$  scale of the EMC ratios is at  $5 \text{ GeV}^2$ .

would play an important role in unveiling the issue on the isospin-dependent nuclear medium effect.

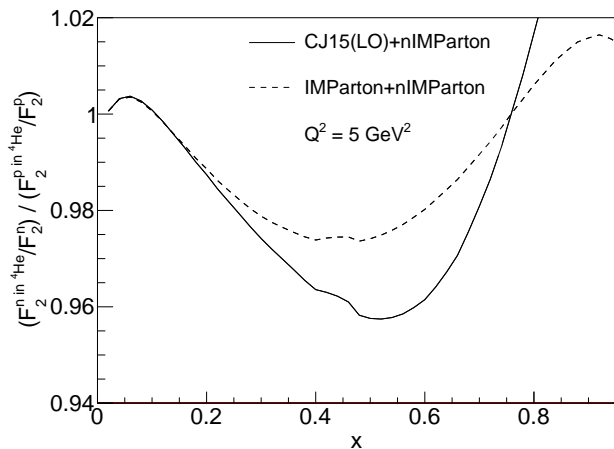


FIG. 8. The ratio of the nuclear modification factor on neutron  $F_2$  to the nuclear modification factor on proton  $F_2$ , for  ${}^4\text{He}$  nucleus. The PDFs of free proton and free neutron are taken from CJ15 [68, 69] and IMParton [70, 71] for the calculations. The nuclear modifications of PDFs in bound nucleons are adopted from nIMParton global analysis [20, 21]. The  $Q^2$  scale of the EMC ratios is at  $5 \text{ GeV}^2$ .

## VIII. SUMMARY

We discussed the new aspect of the EMC effect, the flavor-dependence, using nIMParton nuclear modification factors. The shapes of valence quark distributions are modified according to the Heisenberg uncertainty principle. The nIMParton global analysis assumes the same enlargement of the confinement size for both proton and neutron, and for both up valence quark and down valence quark. Therefore, the isospin-dependence of the EMC effect in the model is due to the fact that the down valence quark distribution is narrower and softer than up valence quark distribution. The CBT model with the isospin-dependent nuclear forces predicts larger nuclear effect difference between up and down quark distributions than that of nIMParton, for heavy nuclei with  $N \neq Z$ .

The flavor-dependent EMC effect based on nIMParton nuclear PDFs is demonstrated with the predictions of various observables in the suggested experiments of PVDIS, pion-induced Drell-Yan, W boson production in p-A collisions, and the tagged-DIS processes. The nIMParton predictions are consistent with the Drell-Yan data decades ago. However we need more experiments in the future to explicitly differentiate various models on EMC effect. The experiment on CLAS12 with the ALERT detector at JLab can be used to test the models on the flavor dependence of the nuclear effect in large  $x$  region, which could provide a timely and critical insight of the new aspect of the EMC effect.

One aim of the ALERT project is to measure the nuclear effect for the mean-field nucleon and the short-range correlated nucleon [24]. With the technique of tagging the recoil nuclei, the EMC effect as a function of nucleon off-shellness can be deduced. In this work, the EMC effect investigated is the average EMC effect of the nucleons. If the confinement enlargement goes up as the local density increasing, the EMC effect should consequently enhanced for the case of high momentum nuclear spectator recoil.

- 
- [1] J. J. Aubert et al. (The European Muon Collaboration), Phys. Lett. B **123**, 275 (1983).  
 [2] M. Arneodo, Phys. Rept. **240**, 301 (1994).  
 [3] D. Geesaman, K. Saito, and A. W. Thomas, Annu. Rev.

- Nucl. Part. Sci. **45**, 337 (1995).  
 [4] P. R. Norton, Rep. Prog. Phys. **66**, 1253 (2003).  
 [5] J. Arrington, A. Daniel, D. B. Day, N. Fomin, D. Gaskell, and P. Solvignon, Phys. Rev. C **86**, 065204 (2012).

- [6] Or Hen, Gerald A. Miller, Eli Piasetzky, and Lawrence B. Weinstein, *Rev. Mod. Phys.* **89**, 045002 (2017).
- [7] S. Malace, D. Gaskell, D. W. Higinbotham, and I. C. Cloët, *Int. J. Mod. Phys. E* **23**, 1430013 (2014).
- [8] R. P. Bickerstaff and G. A. Miller, *Phys. Rev. D* **34**, 2890 (1986).
- [9] K. J. Eskola, V. J. Kolhinen, and P. V. Ruuskanen, *Nucl. Phys. B* **535**, 351 (1998).
- [10] K. J. Eskola, V. J. Kolhinen, and C. A. Salgado, *Eur. Phys. J. C* **9**, 61 (1999).
- [11] J. Seely et al., *Phys. Rev. Lett.* **103**, 202301 (2009).
- [12] L. B. Weinstein, E. Piasetzky, D. W. Higinbotham, J. Gomez, O. Hen, and R. Shneor, *Phys. Rev. Lett.* **106**, 052301 (2011).
- [13] O. Hen, E. Piasetzky, and L. B. Weinstein, *Phys. Rev. C* **85**, 047301 (2012).
- [14] I. C. Cloët, W. Bentz, and A. W. Thomas, *Phys. Rev. Lett.* **109**, 182301 (2012).
- [15] D. Dutta, J. C. Peng, I. C. Cloët, and D. Gaskell, *Phys. Rev. C* **83**, 042201 (2011).
- [16] W. C. Chang, I. C. Cloët, D. Dutta, J. C. Peng, *Phys. Lett. B* **720**, 188 (2013).
- [17] I. C. Cloët, W. Bentz, and A. W. Thomas, *Phys. Lett. B* **642**, 210 (2006).
- [18] I. C. Cloët, W. Bentz, and A. W. Thomas, *Phys. Rev. Lett.* **102**, 252301 (2009).
- [19] W. Bentz, I. C. Cloët, J. T. Londergan, and A. W. Thomas, *Phys. Lett. B* **693**, 462 (2010).
- [20] Rong Wang, Xurong Chen, and Qiang Fu, *Nucl. Phys. B* **920**, 1 (2017).
- [21] <https://github.com/lukeronger/nIMParton>
- [22] W. R. Armstrong, J. Arrington. I. Cloët et al., arXiv:1708.00835.
- [23] W. R. Armstrong, J. Arrington. I. Cloët et al., arXiv:1708.00888.
- [24] W. R. Armstrong, J. Arrington. I. Cloët et al., arXiv:1708.00891.
- [25] C. A. García Canal, E. M. Santangelo, and H. Vucetich, *Phys. Rev. Lett.* **53**, 1430 (1984).
- [26] M. Staszel, J. Rożynek, and G. Wilk, *Phys. Rev. D* **29**, 2638 (1984).
- [27] S. V. Akulinichev, S. Shlomo, S. A. Kulagin, and G. M. Vagradov, *Phys. Rev. Lett.* **55**, 2239 (1985).
- [28] L. L. Frankfurt, M. I. Strikman, *Phys. Lett. B* **183**, 254 (1987).
- [29] Hong Jung and Gerald A. Miller, *Phys. Lett. B* **200**, 351 (1988).
- [30] C. Ciofi degli Atti, L. Kaptari, and S. Scopetta, *Euro. Phys. J. A* **5**, 191 (1999).
- [31] G. V. Dunne and A. W. Thomas, *Phys. Rev. D* **33**, 2061 (1986).
- [32] F. Gross and S. Liuti, *Phys. Rev. C* **45**, 1374 (1992).
- [33] S. A. Kulagin, G. Piller, and W. Weise, *Phys. Rev. C* **50**, 1154 (1994).
- [34] S. A. Kulagin and R. Petti, *Nucl. Phys. A* **765**, 126 (2006).
- [35] S. A. Kulagin and R. Petti, *Phys. Rev. C* **90**, 045204 (2014).
- [36] F. E. Close, R. G. Roberts, and G. G. Ross, *Phys. Lett. B* **129**, 346 (1983).
- [37] R. L. Jaffe, F. E. Close, R. G. Roberts, and G. G. Ross, *Phys. Lett. B* **134**, 449 (1984).
- [38] O. Nachtmann and H. J. Pirner, *Z. Phys. C* **21**, 277 (1984).
- [39] F. E. Close, R. L. Jaffe, R. G. Roberts, and G. G. Ross, *Phys. Rev. D* **31**, 1004 (1985).
- [40] F. E. Close, R. G. Roberts, and G. G. Ross, *Nucl. Phys. B* **296**, 582 (1988).
- [41] R. L. Jaffe, *Phys. Rev. Lett.* **50**, 228 (1983).
- [42] C. E. Carlson and T. J. Havens, *Phys. Rev. Lett.* **51**, 261 (1983).
- [43] M. Chemtob and R. Peschanski, *J. Phys. G* **10**, 599 (1984).
- [44] Gerald A. Miller, *Phys. Rev. Lett.* **53**, 2008 (1984).
- [45] B. C. Clark, S. Hama, B. Mulligan, and K. Tanaka, *Phys. Rev. D* **31**, 617 (1985).
- [46] P. A. M. Guichon, *Phys. Lett. B* **200**, 235 (1988).
- [47] Pierre A. M. Guichon, Koichi Saito, Evgenii Rodionov, and Anthony W. Thomas, *Nucl. Phys. A* **601**, 349 (1996).
- [48] K. Saito, K. Tsushima, and A. W. Thomas, *Prog. Part. Nucl. Phys.* **58**, 1 (2007).
- [49] Ingo Sick, *Phys. Lett. B* **157**, 13 (1985).
- [50] P. B. Siegel, W. B. Kaufmann, and W. R. Gibbs, *Phys. Rev. C* **31**, 2184 (1985).
- [51] G. E. Brown, C. B. Dover, P. B. Siegel, and W. Weise, *Phys. Rev. Lett.* **60**, 2723 (1988).
- [52] Y. Mardor et al., *Phys. Rev. Lett.* **65**, 2110 (1990).
- [53] N. N. Nikolaev, *Z. Phys. C* **32**, 537 (1986).
- [54] Makoto Oka and R. D. Amado, *Phys. Rev. C* **35**, 1586 (1987).
- [55] G. Kälbermann, L. L. Frankfurt, and J. M. Eisenberg, *Phys. Lett. B* **329**, 164 (1994).
- [56] J. Dukelsky, F. Fernández, and E. Moya de Guerra, *J. Phys. G* **21**, 317 (1995).
- [57] Jason R. Smith and Gerald A. Miller, *Phys. Rev. Lett.* **91**, 212301 (2003).
- [58] Jishnu Dey and Mira Dey, *Phys. Lett. B* **176**, 469 (1986).
- [59] V. Barone, M. Genovese, N. N. Nikolaev, E. Predazzi, and B. G. Zakharov, *Z. Phys. C* **58**, 541 (1993).
- [60] L. L. Frankfurt and M. I. Strikman, *Nucl. Phys. B* **250**, 143 (1985).
- [61] Yunhua Zhang, Lijing Shao, and Bo-Qiang Ma, *Nucl. Phys. A* **828**, 390 (2009).
- [62] Arifuzzaman, Pervez Hoodbhoy, and Sajjad Mahmood, *Nucl. Phys. A* **480**, 469 (1988).
- [63] Chr. V. Christov, E. Ruiz Arriola, and K. Goeke, *Nucl. Phys. A* **510**, 689 (1990).
- [64] J. V. Noble, *Phys. Lett. B* **178**, 285 (1986).
- [65] D. M. Alde et al., *Phys. Rev. Lett.* **64**, 2479 (1990).
- [66] M. A. Vasiliev et al. (FNAL E866/NuSea Collaboration), *Phys. Rev. Lett.* **83**, 2304 (1999).
- [67] Ingo Sick and Donal Day, *Phys. Lett. B* **274**, 16 (1992).
- [68] A. Accardi, L. T. Brady, W. Melnitchouk, J. F. Owens, and N. Sato, *Phys. Rev. D* **93**, 114017 (2016).
- [69] <https://www.jlab.org/theory/cj/>
- [70] Rong Wang and Xu-Rong Chen, *Chinese Physics C* **41**, 053103 (2017).
- [71] <https://github.com/lukeronger/IMParton>
- [72] P. Bordalo et al. (NA10 Collaboration), *Phys. Lett. B* **193**, 368 (1987).
- [73] J. Badier et al. (NA3 Collaboration), *Phys. Lett. B* **104**, 335 (1981).
- [74] M. Corden et al., *Phys. Lett. B* **96**, 417 (1980).
- [75] N. Baillie et al. (CLAS Collaboration), *Phys. Rev. Lett.* **108**, 142001 (2012).
- [76] N. Baillie et al. (CLAS Collaboration), *Phys. Rev. Lett.* **108**, 199902 (2012).
- [77] S. Tkachenko et al. (CLAS Collaboration), *Phys. Rev. C*



89, 045206 (2014).